

IMECE2009-10053

Automotive Lifts – Unrestrained v. Restrained Swing Arms

Ralph L. Barnett

Triodyne Inc.

450 Skokie Boulevard, Suite 604

Northbrook, IL 60062

(847) 677-4730, Fax (847) 647-2047

infoserv@triodyne.com

John B. Glauber

Student

University of Illinois at Urbana-Champaign,

Materials Science and Engineering

ABSTRACT

To perform automotive maintenance, there are many makeshift ways of lifting and holding a vehicle including the use of forklifts, overhead hoists and cranes, jacks of every kind, jack stands and various ramp systems. When automobiles fall from these devices, the causes are usually obvious and we disapprovingly tolerate the risk taking. On the other hand, when a vehicle falls from a dedicated automotive lift, the accident is entirely unacceptable. This paper examines several hidden dangers associated with a particular class of lifts that are “frame engaging.” Various styles of these lifts use four cantilevered arms to elevate and support vehicles on adapter pads positioned on the arms’ free ends. If the vehicle slides off of one or more pads, it usually falls catastrophically. The cantilevered arms, when raised, are supposed to be restrained against rotation in a horizontal plane. When restrained, the arms provide a robust structural system for resisting horizontal workplace forces that tend to slide vehicles off the pads. The arms maintain the horizontal locations of the adapters by developing bending and axial planar resistance. If, on the other hand, the arms are free to pivot due to sloth or poor design, their structural behavior is dramatically transformed. The planar bending resistance of the arms completely disappears and they become direct stress diagonal truss members; the vehicle itself unwittingly becomes the truss’ tension chord. The appearance of the fixed and pivoting systems is the same; however, the truss action magnifies the horizontal forces acting on the adapter pads increasing the slip probability. Indeed, depending on the orientation of the pivoting swing arms, any finite horizontal force applied to a vehicle may lead to an unbounded tangential “slide-out” force. This is, of course, a theoretical possibility, not a practical reality.

INTRODUCTION

The automotive lift illustrated in Fig. 1 supports vehicles at their lift points by four adapter pads attached to the free ends of four swing arms operating in an elevated plane. The swing arms are telescoping and pivoting to enable a mechanic to locate the

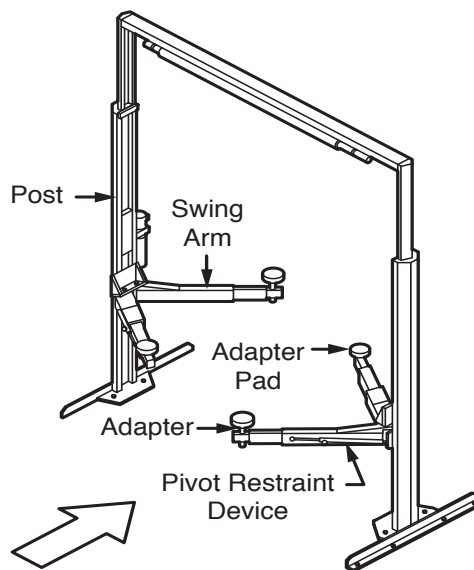
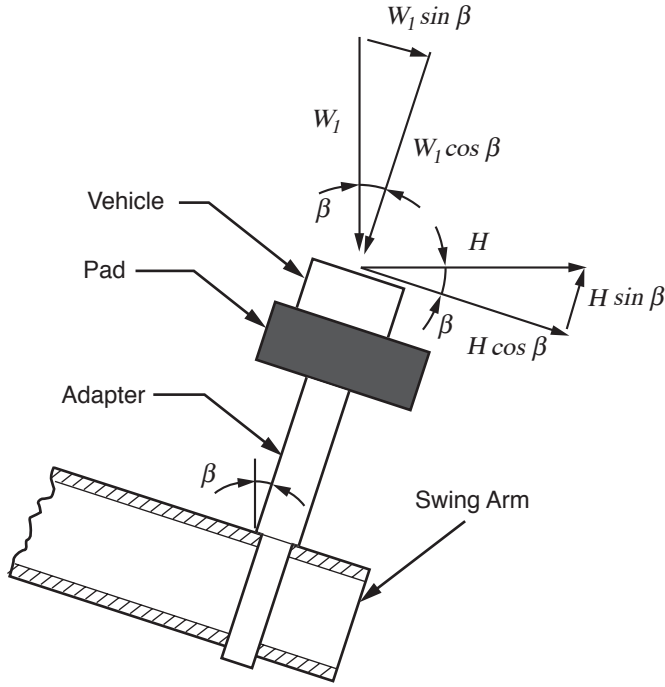


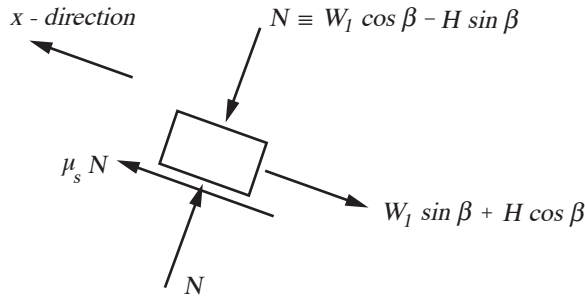
Figure 1. Two Post, Frame Engaging, Clear Floor Surface Mounted Automotive Lift

adapters beneath the lift points when the vehicle rests on the floor surface. When a vehicle is elevated, its stability requires, among other things, that the planar locations of the adapters be maintained throughout a loading history characterized by vibration, changing positions of the center of gravity, deflecting swing arms, distortion of the vehicle structure and applied horizontal and vertical forces and moments. These latter forces are generated manually by one or more mechanics working on the vehicle; the vehicles are not operating while suspended.

Adapters are not clamped to the vehicle; they are not inserted into interference devices such as saddles or detents. They retain their positions relative to the lift points by three mechanisms; adapter pad friction resistance, pivot arm restraint devices and telescoping arm friction resistance. Unfortunately, these mechanisms are not straightforward which accounts in no small measure for the tragic excursions involving falling vehicles.



a) Tilted Adapter



b) Free Body Diagram

Figure 2. Friction Analysis of Deflected Swing Arm

Adapter Pad Frictional Resistance

Tangential resistance is developed between the adapter pads and the vehicle lift points; for very stiff swing arms, this frictional resistance is the product of the pad loading W_1 and the coefficient of static friction μ_s for the pad/lift point interface. For flexible swing arms, the adapter and pads will tilt away from the vertical by an angle β when supporting a vehicle as shown in Fig. 2. This case is analyzed using classic friction theory.

The “no slip” formulation involves the summation in the x-direction of the forces shown in the free body diagram, Fig. 2-b. Thus,

$$(W_1 \cos \beta - H \sin \beta) \mu_s \geq W_1 \sin \beta + H \cos \beta \dots \text{no slip}$$

or

$$H \leq W_1 \left[\frac{\mu_s - \tan \beta}{1 + \mu_s \tan \beta} \right] \quad (1)$$

where H is the applied horizontal force acting at the adapter. When $H = 0$, we obtain the familiar result,

$$\mu_s \geq \tan \beta \dots \text{no slip} \quad (2)$$

The bracketed expression in Eq. 1 becomes the tilted pad/lift point friction coefficient μ_t . For example, when $\beta = 5^\circ$ and $\mu_s = 0.7$,

$$\mu_t = \frac{0.7 - \tan 5^\circ}{1 + (0.7) \tan 5^\circ} = 0.577$$

Note that,

$$\mu_t \leq \mu_s \quad (3)$$

In addition to swing arm deflection, frictional resistance may also be compromised by contamination on the adapter pad/lift point interface. Without belaboring the issue, when the vehicle is on the road, the lift points are exposed to road contaminants; and the adapter pads live in a garage environment filled with lubricants and liquid hydrocarbons that are slippery.

Effective cleaning of the interface requires an aggressive protocol involving solvents and abrasion of the surfaces. In practice, the problem of contamination is usually ignored; sometimes a dry wiper rag is applied. Notwithstanding this inattention, contamination produces a first order effect on tangential pad resistance; it may increase or decrease the resistance to lateral loads.

The hyperstatic nature of the automotive lift’s “four point support system” gives rise to another major effect on the frictional resistance of the adapter pad/lift point interface. This subtle phenomenon was discussed in the paper, “Vehicle Lifts: The Hyperstatic Problem” [1]. In essence, one can only state that the sum of the four vertical pad reactions must equal the weight of the vehicle; the distribution of forces among the pads cannot be determined. Furthermore, one or two pads may carry zero load. Obviously, this implies that the tangential resistance of any pad may be as low as zero since frictional resistance is proportional to the normal force acting on the pad. A low pad force is undetectable without instrumentation. Zero pad forces may manifest themselves by

rocking of the vehicle in the same way that a table rocks when one leg is “too short.”

Swing-Arm-Pivot Restraint

Elevated swing arms are supposed to be restrained against rotation in the horizontal plane. This requirement may be found, among other places, in the American National Standard for Automotive Lifts – Safety Requirements for Construction, Testing and Validation, ANSI/ALI ALCTV:2006. [2]:

9.2.8 Swing Arms

Lifts incorporating two superstructures with a clearance dimension of fifty-one (51) inches or greater between superstructures shall require swing-arm-pivot restraints.

Swing-arm-pivot restraints shall be normally engaged at all heights above two and one-half (2-1/2) inches of the lift lowest position for lifts with a rated capacity of fifteen thousand (15,000) pounds or less, and four (4) inches of the lift lowest position for lifts with a rated capacity above fifteen thousand (15,000) pounds.

Swing-arm-pivot pins shall incorporate means to inhibit unintentional removal or disengagement.

7.6 Arm Restraint

A device that maintains the pivotal position of a swing arm after the swing arm and adapter have been set for proper vehicle engagement, and prior to contact with the vehicle lifting points.

9.1.1.5 Strength of Swing-Arm-Pivot Restraints

Frame engaging lifts not having a rigid superstructure, or portion thereof, under the raised vehicle shall be provided with swing-arm-pivot restraints capable of resisting a horizontal force of one hundred fifty (150) pounds without permanent deformation, when applied at the end of the fully extended, unloaded arm.

Consider, for example, the restraint mechanism shown in Fig. 3. When properly set in a field test recently conducted, the adapter end of the arm moved laterally through a range of 7.5 in. Furthermore, the locking system was designed so it could be intentionally disabled allowing the arm to pivot through 180°. The principle focus of this paper is to expose the downside of the pivoting action however it arises. In our previous paper on hyperstatic behavior [1], it was demonstrated that a near-zero loading of an adapter makes the

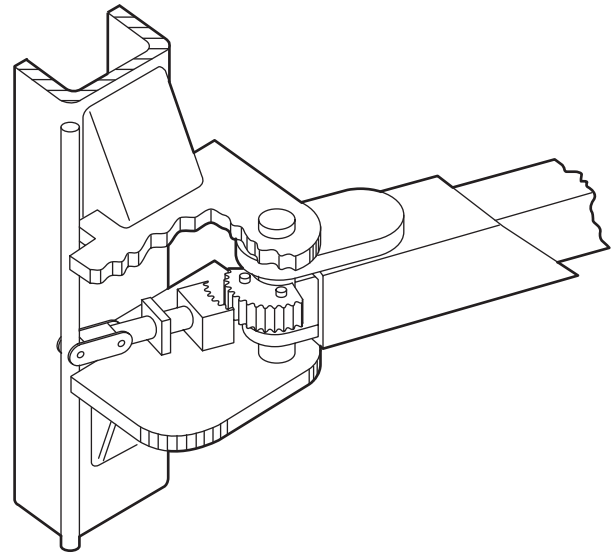


Figure 3. Gear-type Swing Arm Restraint Mechanism

positional integrity of the swing arms vulnerable to accidental bumping. Here, we show that pivoting capability dramatically magnifies the sideways forces applied to the adapter sites which tend to push vehicles off their lift points.

All automotive lift standards prohibit swing arm pivoting including ANSI/ALI ALCTV:2006 [2], ANSI B153.1-1990 [3]; British Standard BS EN 1493:1999 [4] and the German Accident Prevention Regulation: Lifting Platforms, VBG 14: April 1, 1977 and January 1, 1995 [5]. Only the latter contains an exculpatory instruction;

Section 17(1):

Implementation instruction: [1]

Movements of the loading device caused by its construction to compensate for small angle and rigging up inaccuracies are not considered swinging, unintentional tilt, rotation or shift.

This instruction was ill-advised.

Telescoping Arm Friction Resistance

When a vehicle is resting on the floor, the telescoping swing arms shown in Fig. 1 are manually maneuvered beneath the vehicle lift points. Telescoping is easily performed. When the vehicle is lifted and a load W_1 acts on the adapter pad shown in Fig. 4, the telescoping motion is resisted by friction; the maximum breakaway force P is given by:

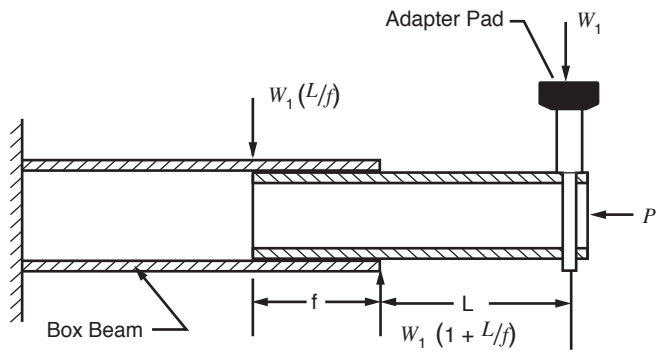


Figure 4. Telescoping Swing Arm

$$P = \mu_b W_1 [1 + 2(L/f)] + \mu_b W_b (L/f) \quad (4)$$

where μ_b is the coefficient of friction between the steel box beams and W_b is the weight of the inside box beam.

The ANSI/ALCTV:2006 standard does not require mechanical locking against telescoping. Nor does the German Accident Prevention Regulation; Lifting Platforms; VBG 14; January 1, 1995 except when the telescoping elements are in roller guides. On the other hand, the British Standard for Vehicle Lifts, BS EN 1493:1999, requires that vehicle lifts be provided with automatic devices to prevent inadvertent motion of the swing arms (see Sections: 5.7.2; 5.8.1; 5.8.5) [4].

HORIZONTAL RESISTANCE

The lift arms illustrated in Fig. 5 represent restrained swing arms which shall be designated rigid. The adapter pads, which are free to rotate about a vertical axis, derive no special properties from being affixed to rigid cantilevers; indeed, any rigid pylons or pedestals provide equivalent support. The four maximum friction force vectors shown in Fig. 5 act on the vehicle and equilibrate the external force $4P_r$ acting on the vehicle supported on the rigid arms, i.e.,

$$4P_r = \mu W_1 + \mu W_2 + \mu W_3 + \mu W_4$$

or

$$P_r = \frac{\mu W}{4} \dots \text{maximum resistance} \quad (5)$$

where W is the total vehicle weight, μ is a deterministic value of the coefficient of friction acting between the adapter pads and the vehicle lift points, and the weights W_1 , W_2 , W_3 and W_4 are the weights distributed among the adapter pads. The actual weight

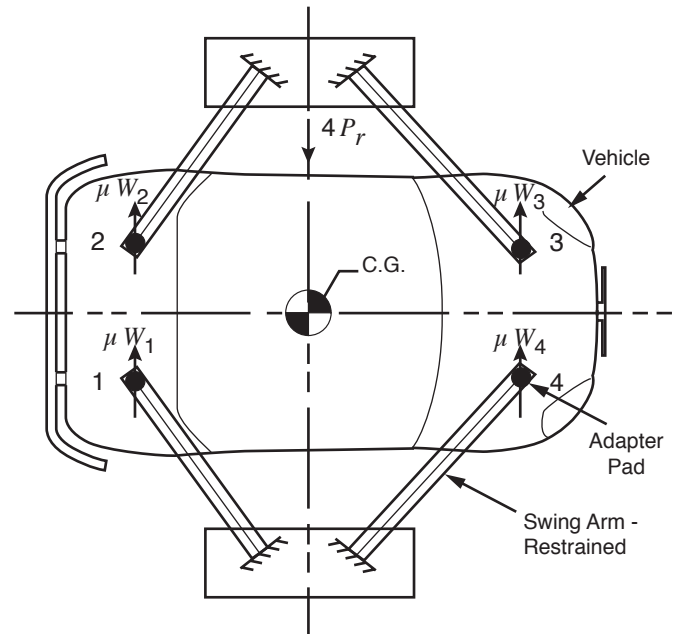


Figure 5. Rigid and Restrained Swing Arms

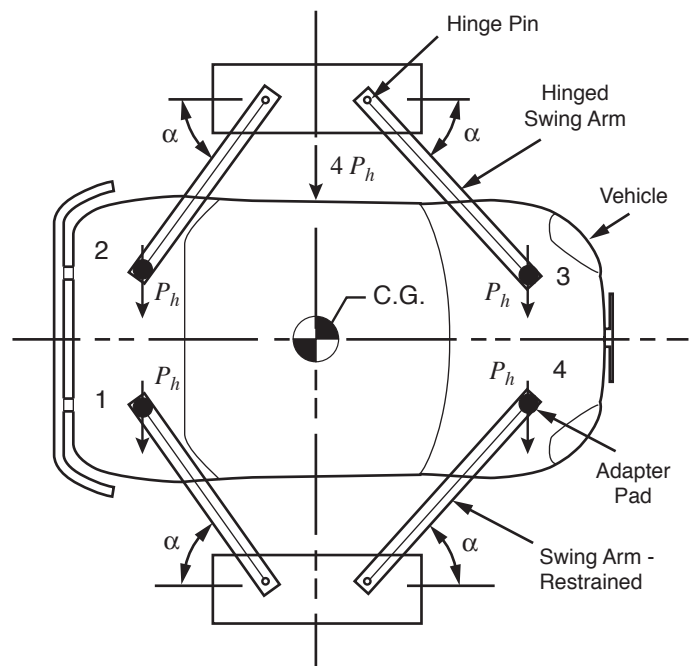


Figure 6. Hinged Swing Arms

distribution cannot be determined by analysis; their total must be W to satisfy vertical equilibrium. Incipient sliding occurs simultaneously at the four pads.

The symmetrically loaded vehicle lift depicted in Fig. 6 represents a lift model with hinged swing arms, each of which is subjected to an external load P_h . The hinged condition is realized when

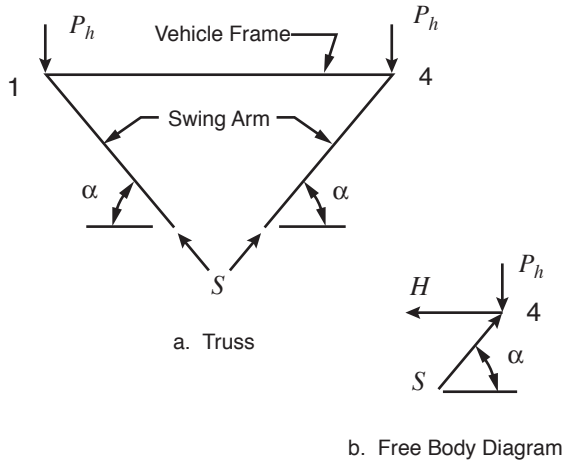


Figure 7. Structural Model

the swing locks are bypassed or when impoverished fixity from poor design or faulty maintenance is encountered. Because the adapter pads are hinged, the ideal truss structure shown in Fig. 7a is obtained where the vehicle frame acts as a “two force” member between the two adapter pads. Referring to the free body diagram in Fig. 7b, horizontal equilibrium requires that,

$$P_h = S \sin \alpha \quad (6)$$

and

$$H = S \cos \alpha \quad (7)$$

where $4P_h$ is the vehicle loading on the hinged lift and $0 \leq \alpha \leq 90^\circ$. Equation 7 implies that $H \leq S$. Equation 6 becomes:

$$S = P_h / \sin \alpha$$

which demonstrates that $S \geq P_h$. Consequently, as the loading P_h increases, the tangential force S at the lift point will eventually equal the maximum frictional resistance at the pads; thus,

$$S = P_h / \sin \alpha \leq \mu W / 4 \dots \text{no slip} \quad (8)$$

where uniform pad loading is assumed. Thus, the maximum lateral loading P_h that urges the vehicle lift points to slide off of the adapter pads is,

$$P_h = \frac{\mu W}{4} \sin \alpha$$

or using Eq. 5,

$$P_h / P_r = \sin \alpha \approx \alpha \quad (9)$$

Table I. Horizontal Resistance Ratio P_h/P_r Hinged Arms /Fixed Arms

Arm Orientation α (degrees)	Resistance Ratio $P_h / P_r = \sin \alpha$	Reciprocal Ratio $P_r / P_h = \text{cosec } \alpha$
Zero	0	∞
10	0.174	5.76
15	0.259	3.86
20	0.342	2.92
25	0.423	2.37
30	0.500	2
35	0.574	1.74
40	0.643	1.56
45	0.707	1.41
90	1.000	1

where the approximation is accurate for small angles (zero to $\pi/5$) and where α is expressed in radians. Table I tabulates the dramatic reduction in lateral resistance occasioned by the rotational capability of the swing arms.

The disadvantage of the hinged swing arms is even more radical than revealed in Table I. When the arms are rigid, slipping occurs simultaneously among the four adapter pads. With hinged arms, slipping may occur at a single pad while the remaining pads are unchallenged by incipient slip. The analysis of the swing arms may be reformulated to reflect the stochastic nature of friction and the indeterminate state of the pad loading. Referring to Fig. 8, the i^{th} pad carries the weight W_i and is characterized by a coefficient of friction μ_i ; the maximum frictional drag force is $(\mu_i W_i)$. As described by Eq. 8, this drag force provides a bound on the applied force $(P_h)_i$ when W_i replaces $W/4$ and μ_i replaces μ ; thus,

$$(P_h)_i \leq (\mu_i W_i) \sin \alpha \quad (10)$$

Returning to Fig. 8, when the vehicle is symmetrically loaded by a horizontal force $4P_h$, each of the adapter pads is exposed to a horizontal force P_h . As P_h increases, one of the pads will allow its lift point to slip; this pad will have the lowest maximum drag $(\mu_i W_i)$, say $(\mu_i W_i)^{\min}$ with the associated loading $(P_h)_i^{\min}$. Thus, the horizontal vehicle loading $4P_h$ that will cause a lift point to slip off its adapter pad is,

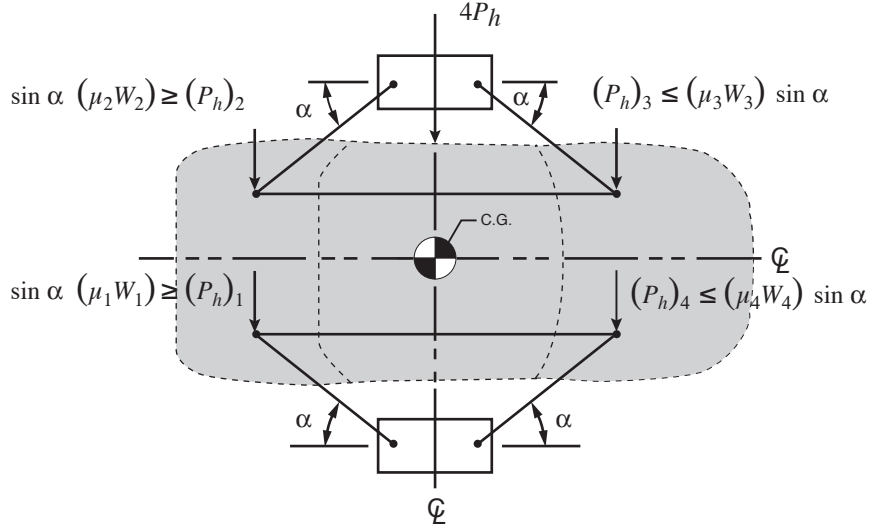


Figure 8. Symmetrical Horizontal Loading of Hinged Arms

$$4P_h = 4(P_h)_i^{\min} = 4(\mu_i W_i)^{\min} \sin \alpha \quad (11)$$

The corresponding resistance of the four rigid arms is

$$4P_r = \bar{\mu} W \quad (12)$$

where $\bar{\mu}$ is the average friction coefficient for the pad/lift point couples; [i.e., $\bar{\mu} = (\mu_1 + \mu_2 + \mu_3 + \mu_4) / 4$]. Consequently,

$$P_h / P_r = \left[\frac{4(\mu_i W_i)^{\min}}{\bar{\mu} W} \right] \sin \alpha = \frac{\mu_{\text{eff}}}{\bar{\mu}} \sin \alpha \quad (13)$$

where $4(\mu_i W_i)^{\min} / W$ is the effective friction drag coefficient on the hinged arms, μ_{eff} .

The bracketed quantity is always less than unity because the average friction drag force $\bar{\mu}(W/4)$ is always greater than the smallest friction drag force $(\mu_i W_i)^{\min}$.

The objective of this paper was to establish Eq. 13 which expresses the diminished horizontal resistance of hinged arms compared to fixed or rigid arms. The ratio P_h / P_r is proportional to $\sin \alpha$ which ranges from zero to unity and reflects the magnified adapter pad loading that arises from the “truss” behavior of the hinged arms. The ratio is also proportional to the bracketed quantity of Eq. 13 that also ranges from zero, when an arm is load free ($W_i = 0$), to unity for ideal behavior when μ is deterministic ($\mu_i = \bar{\mu}$) and the vehicle weight distribution is uniform ($W_i = W/4$). The bracketed quantity accounts for the propensity of the hinged arms to seek out the pad with the weakest drag resistance.

TESTING

A series of experiments were conducted to explore the differences in behavior between rigid and hinged swing arms. To mimic a two-post frame engaging automotive lift, the fixture illustrated in Fig. 9 was constructed with four aluminum swing arms with sensitive pivot bearings that allow the arms to swing in a horizontal plane by gently blowing on them. Thumb screws were used to steady the arms during set-up, photographing and videotaping; they were disconnected during test runs. The miniature adapter

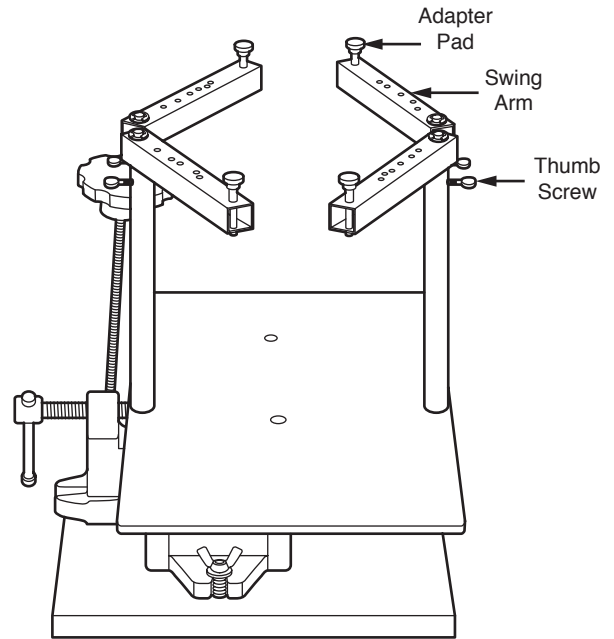


Figure 9. Four Arm Test Fixture-Horizontal

pads rotated in situ and were fabricated with neoprene pads. The base of the fixture could be tilted as depicted in Fig. 10. To restrain the four swing arms at predetermined angles ($\alpha = 15^\circ, 20^\circ, 25^\circ, 30^\circ$ and 35°), a predrilled aluminum plate was secured to the arms by four screws during testing, Fig. 11. This plate was also used as a template for setting the swing arm angles during the hinged or unrestrained testing program. Before testing, the aluminum plate was screwed into the arms at a selected swing arm angle, the specimen was supported by the arms and the aluminum plate was unscrewed and removed.

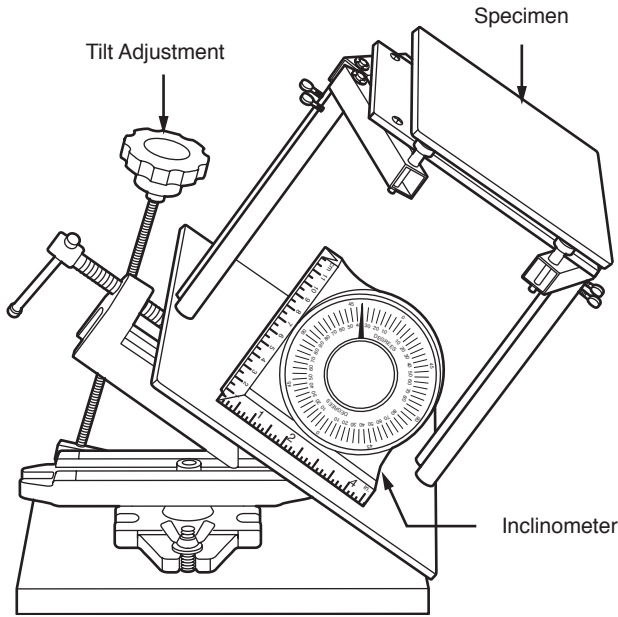


Figure 10. Tilted Test Fixture

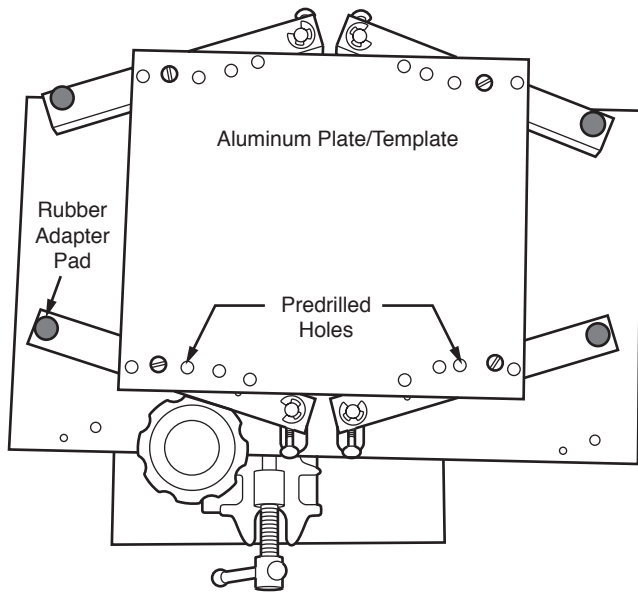


Figure 11. Aluminum Restraint Plate and Template

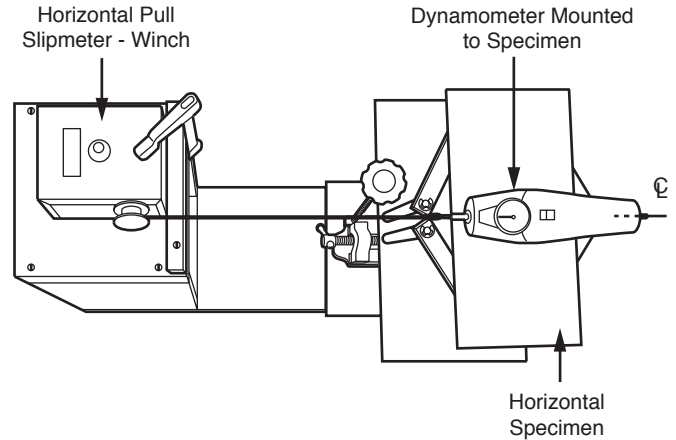


Figure 12. Horizontal Pull Test Fixture

Pull Test

To measure the horizontal drag resistance of a specimen, a Horizontal Pull Slipmeter manufactured by Whiteley Industries was mounted alongside the test fixture shown in Fig. 12. The test specimens were either a mild steel plate or a plastic plate which were attached to a dynamometer. Following classic slip test protocol as specified by ASTM F609-79 [6], a slow speed winch pulled on a horizontal string hooked to the dynamometer until slip was detected at one of the adapter pads. The associated pull was recorded for each test after it was repeated ten times. Before each test, specimens were cleaned with seventy percent isopropyl rubbing alcohol, the adapter pads were lightly sanded and blown with a pressurized gas duster (Cinnovera). The tests were performed with hinged and fixed swing arms at five swing arm angles and at corresponding lift point locations. The data are presented in Tables II and III. A separate set of tests were conducted after placing oil on the steel plate. Before performing the tests, the oil was wiped off and the pads were lightly sanded and blown with a pressurized duster. The data associated with the oiled plates are presented in Table IV.

Tilt Tests

The horizontal pull tests were conducted by subjecting a steel or plastic plate to a single symmetrical horizontal pull force applied when the specimen was supported on four symmetrical arms. The forces that cause slipping were recorded and converted into friction coefficients. The steel plate specimens were also tested on a tilt fixture where a symmetrical body force was generated. Here, the smallest tilt angles were recorded that gave rise to slipping; the tangents of these angles are the friction coefficients which are summarized in Table V. For each of the five arm orientations corresponding to the horizontal pull tests, ten tilt tests were conducted for the hinged and fixed swing arms; their associated tilt angles are tabulated in Table V. The specimen weight is not required for determining the friction coefficients when using the tilt test. Note that gravity acts on both the specimen and the light weight aluminum arms.

When the swing arms are fixed, the traditional pull tests and tilt tests should give equivalent coefficients of friction. Observe in Table II that the mean friction coefficient for fifty fixed arm horizontal pull tests is 0.698 with a standard deviation of 0.0175; the corresponding 50 tilt tests tabulated in Table V produced a mean friction coefficient of 0.6835 with a standard deviation of 0.0440.

CONCLUSIONS AND DISCUSSION OF RESULTS

To prevent a vehicle from falling off of an elevated automotive lift, the cantilever supported adapter pads must not slide from under the vehicle lift points. This paper shows that hinged behavior of the cantilever lift arms severely compromises the ability of the adapter pads to maintain contact with the vehicle. Rotation of the arms modifies the structural behavior which dramatically magnifies the lateral pad escape forces. Furthermore, the hinge action prevents the four pads from working together and causes the “weakest link” pad to control the resistance to slide-off.

A. The behavior of hinged automotive lift swing arms relative to fixed (restrained) arms is revealed by plotting the lateral resistance ratios given by P_h/P_r or equivalently by $\mu_{eff}/\bar{\mu}$ against the sine of the arm orientation angle, $\sin \alpha$. These ratios are tabulated in Tables II through V; they reflect the inefficiency of the hinged arms compared to the rigid arm resistance. Four graphs of P_h/P_r are presented in Figs. 13 through 16 for the following cases:

Fig. 13 - Horizontal Pull Test: 6.729 lb - steel plate specimen

Fig. 14 - Tilt Test: 5.320 lb - steel plate specimen

Fig. 15 - Horizontal Pull Test: 3.760 lb - cast acrylic plastic plate specimen

Fig. 16 - Horizontal Pull Test: 6.729 lb - lubricated steel plate specimen (Exxon Superflo 10W-30)

B. Each of the four graphs present two curves. The higher curve with the equation $P_h/P_r = \sin \alpha$ represents the inefficiency of the hinged arms caused by the deterministic increase in horizontal adapter pad loading associated with truss behavior as opposed to the cantilever action of the fixed swing arms. Because the $\sin \alpha$ was chosen as the independent variable, the curve is a straight line through the origin. The slope of this curve is unity; the intercept is zero. For shallow swing arm angles that approach zero, the $\sin \alpha$ approaches zero and the lateral resistance of the hinged arms approaches zero.

C. The lower curves in each of the four graphs indicate that the resistance ratio P_h/P_r is proportional to both the $\sin \alpha$ and the indicated slope $[(\mu_i W_i)^{min} / (\bar{\mu} W / 4)]$ which is never greater than unity. This slope contains three random variables; μ_i , $\bar{\mu}$ and W_i . It is remarkable that it is so stable over the

range of α ; note that the coefficients of determination, R^2 , are almost unity for all four plotted curves in the graphs [7].

The slope of the four lower curves reflects the notion that the hinged arms seek out the adapter pad with the smallest lateral resistance compared to the average pad resistance provided by the four fixed arms. The slope of these curves represents an additional reduction in the inefficiency of the hinged arms over the deterministic inefficiency represented by the upper curves. This physical interpretation of the slope was made possible by the choice of $\sin \alpha$ as the independent variable. Taking (1 - slope) expressed as a percentage, we observe that the additional reductions in the four case graphs are:

26.5% . . . Horizontal Pull Test - steel specimen

19.3% . . . Tilt Test - steel specimen

26.0% . . . Horizontal Pull Test - (cast plastic) acrylic specimen

24.7% . . . Horizontal Pull Test - lubricated steel specimen (Exxon Superflo 10W-30)

As an example, the steel plate in Fig. 13 shows a 50% reduction in the deterministic resistance of hinged arms with $\alpha = 30^\circ$ (top curve); combined with the stochastic inefficiency, the lower curve indicates that the hinged arms have only 36% of the resistance of the fixed arms.

Unfortunately, there is presently no analytic method for predicting the slope of the P_h/P_r diagram for a specific automotive lift installation and vehicle. The laboratory studies have shown, however, that stochastic behavior of the hinged arms is significant and measurable.

D. The tilt tests of the steel specimen produced a greater slope (Fig. 14) than the corresponding horizontal pull tests (Fig. 13). Consider some of the physical differences in the test profiles:

- The tilt test employs gravitational body forces; the horizontal pull test loads the specimen by traction forces and moments that tend to pitch the plate.
- Body force tends to swing the hinged arms in the tilt test.
- The specimen weight is greater in the horizontal pull test.
- The out-of-plane bending of the swing arms is smaller in the tilt test.

Maybe the uniformity of the tilt test gave rise to its greater slope in the P_h/P_r diagram.

E. The combination of hinged swing arms and a small orientation angle leads to a dangerous reduction in a vehicle’s horizontal resistance to sideways forces. Various factors may produce shallow angles:

- Fully extended telescoping arms

- Very wide vehicles
- Lift points along the outer edges of the vehicle
- Vehicles not centered between the posts
- Skewed (yawed) vehicles

These factors have little effect when the swing arms are fixed.

- F. Proper design should provide sufficient swing arm restraint to eliminate hinge behavior of the swing arms. Even small rotations may overcome the static friction and then give rise to the lower levels of dynamic friction.

REFERENCES

- [1] “Barnett, Ralph and Peter J. Poczynok, “Vehicle Lifts: The Hyperstatic Problem,” Triodyne Safety Brief, Vol. 13, No. 2, August 1997.
- [2] American National Standard for Automotive Lifts – Safety Requirements for Construction, Testing and Validation, ANSI/ALI ALCTV: 2006.
- [3] ANSI B153.1-1990; Automobile Lifts-Safety Requirements for the Construction, Care and Use.
- [4] British Standard BS EN 1493: 1999.
- [5] German Accident Prevention Regulation: Lifting Platforms, VBG 14: April 1, 1977 and January 1, 1995.
- [6] American Society for Testing and Materials (ASTM), (1989b) – Standard Test Method for Static Slip Resistance for Footwear, Sole, Heel, or Related Materials by Horizontal Pull Slipmeter (HPS), ASTM F609-79, 1989.
- [7] Devore, Jay L., “Probability and Statistics for Engineering and the Sciences,” Chapter 12, p. 506, 2000.

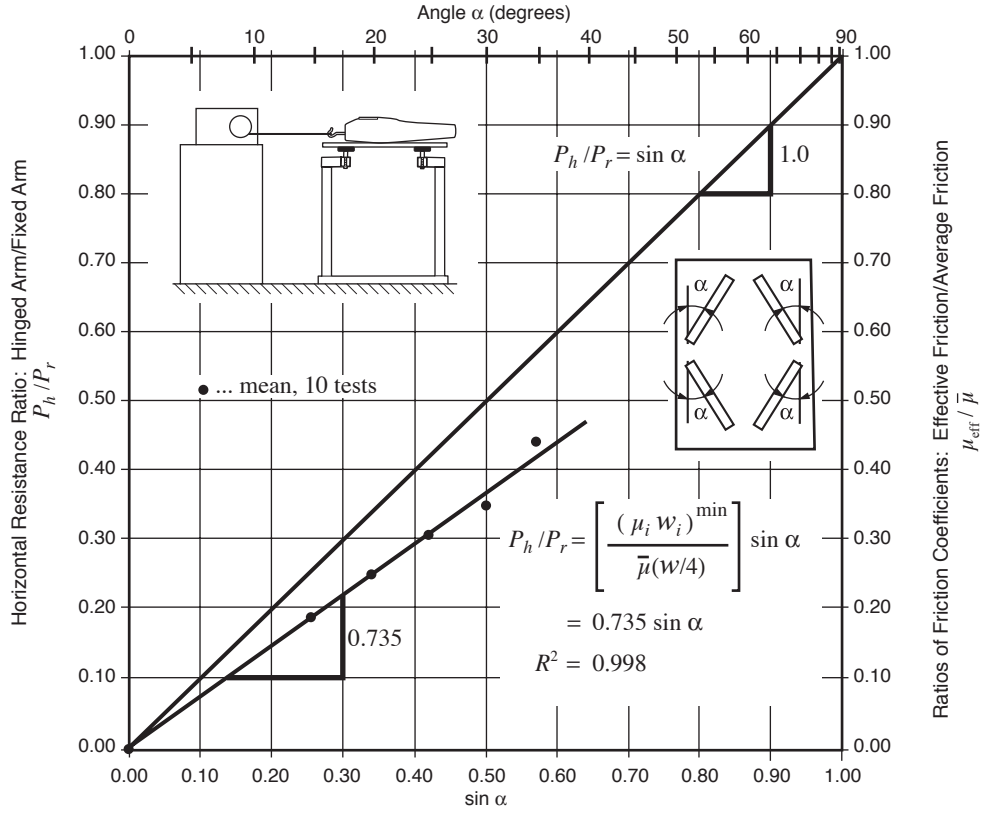


Figure 13. Horizontal Pull Test - Steel Plate

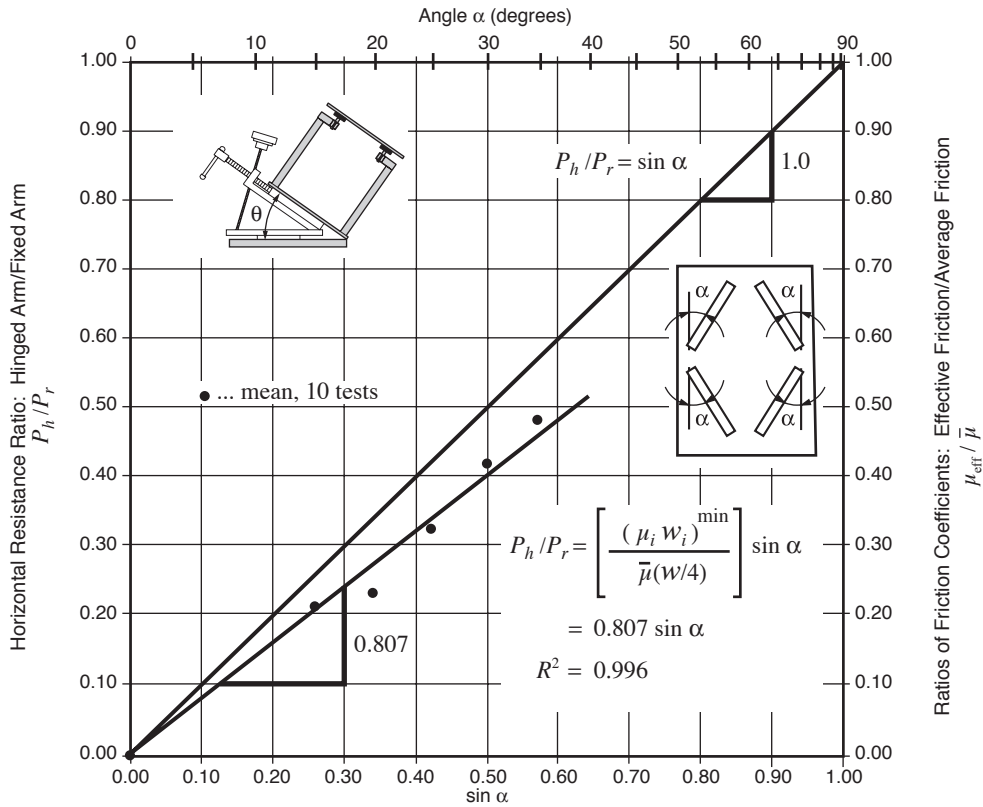


Figure 14. Tilt Test - Steel Plate

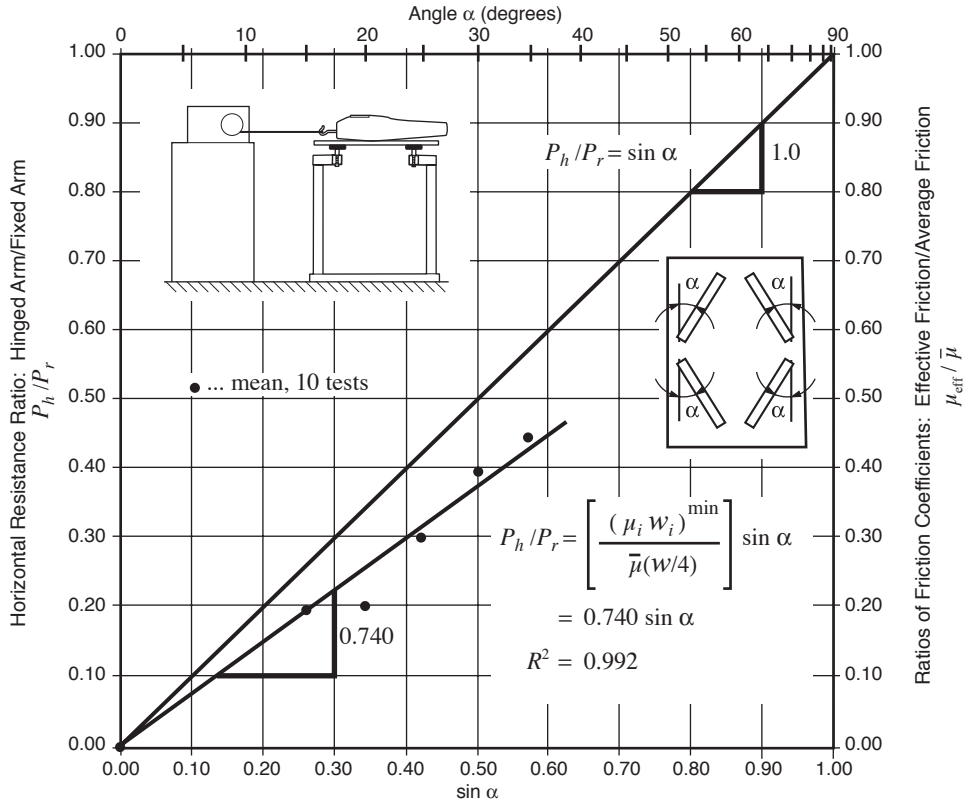


Figure 15. Horizontal Pull Test - Plastic Plate (Cast Acrylic)

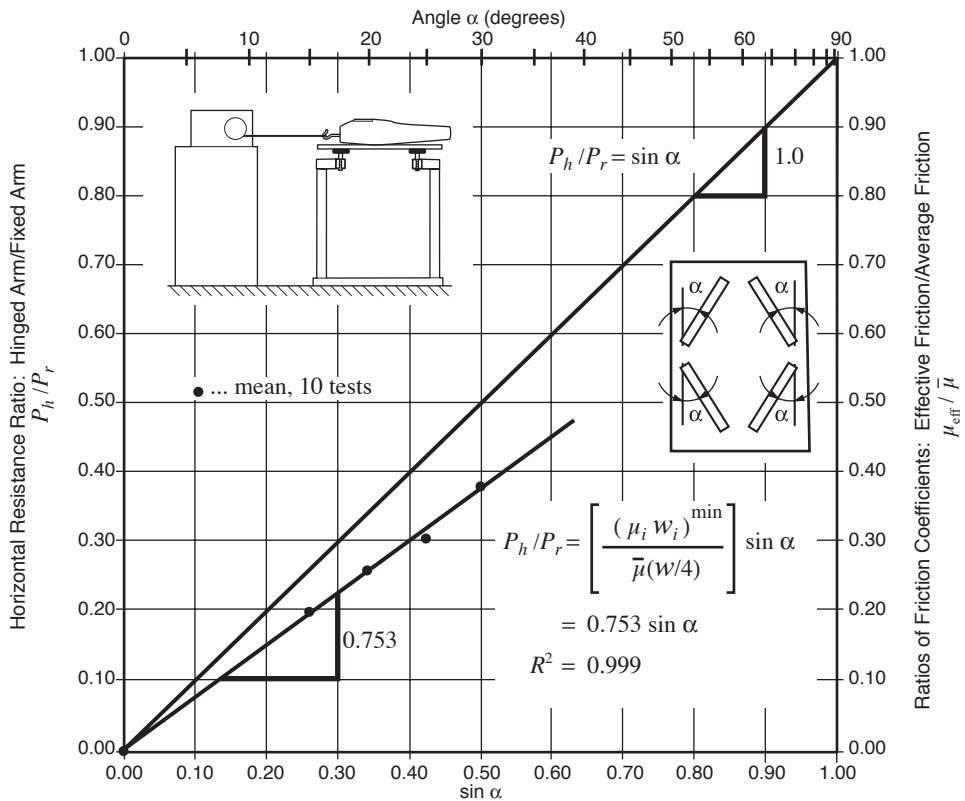
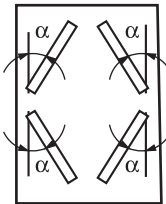
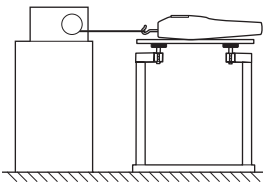


Figure 16. Horizontal Pull Test - Lubricated Steel Plate / Exxon Superflo 10W-30

APPENDIX - Test Data

Table II. Horizontal Pull Test Data
Steel Plate - Wt. 6.729 lbs

Trial Number	Arm Orientation α (degrees)	Frictional Force (lb) P_r Fixed Arms	Average Friction Coefficient $\bar{\mu} = P_r / W$	Frictional Force (lb) P_h Hinged Arms	Average Friction Coefficient $\mu_{eff} = P_h / W$	$\mu_{eff} / \bar{\mu}$
1	15	4.82	0.716	0.82	0.122	
2	15	4.79	0.712	0.95	0.141	
3	15	4.88	0.725	0.79	0.117	
4	15	4.81	0.715	0.91	0.135	
5	15	4.88	0.725	0.85	0.126	
6	15	4.79	0.712	0.89	0.132	
7	15	4.87	0.724	1.09	0.162	
8	15	4.62	0.687	0.82	0.122	
9	15	4.72	0.701	0.89	0.132	
10	15	4.76	0.707	1.00	0.149	
Average (Mean)		4.79	0.712	0.90	0.134	0.188
Standard Deviation		0.081	0.012	0.092	0.014	
1	20	4.82	0.716	1.12	0.166	
2	20	4.52	0.672	1.18	0.175	
3	20	4.50	0.669	1.21	0.180	
4	20	4.69	0.697	1.09	0.162	
5	20	4.68	0.695	1.22	0.181	
6	20	4.61	0.685	1.19	0.177	
7	20	4.69	0.697	1.13	0.168	
8	20	4.59	0.682	1.09	0.162	
9	20	4.60	0.684	1.06	0.158	
10	20	4.59	0.682	1.23	0.183	
Average (Mean)		4.63	0.688	1.15	0.171	0.249
Standard Deviation		0.094	0.014	0.061	0.009	
1	25	4.71	0.700	1.36	0.202	
2	25	4.69	0.697	1.49	0.221	
3	25	4.89	0.727	1.32	0.196	
4	25	4.89	0.727	1.69	0.251	
5	25	4.61	0.685	1.49	0.221	
6	25	4.71	0.700	1.39	0.207	
7	25	4.70	0.698	1.49	0.221	
8	25	4.88	0.725	1.36	0.202	
9	25	4.61	0.685	1.39	0.207	
10	25	4.62	0.687	1.51	0.224	
Average (Mean)		4.73	0.703	1.45	0.215	0.306
Standard Deviation		0.114	0.017	0.109	0.016	
1	30	4.86	0.722	1.78	0.265	
2	30	4.69	0.697	1.62	0.241	
3	30	4.68	0.695	1.59	0.236	
4	30	4.62	0.687	1.60	0.238	
5	30	4.75	0.706	1.79	0.266	
6	30	4.53	0.673	1.67	0.248	
7	30	4.52	0.672	1.65	0.245	
8	30	4.55	0.676	1.49	0.221	
9	30	4.57	0.679	1.49	0.221	
10	30	4.61	0.685	1.50	0.223	
Average (Mean)		4.64	0.689	1.62	0.241	0.350
Standard Deviation		0.108	0.016	0.109	0.016	
1	35	4.72	0.701	2.09	0.311	
2	35	4.62	0.687	2.00	0.297	
3	35	4.87	0.724	1.95	0.290	
4	35	4.73	0.703	2.19	0.325	
5	35	4.68	0.695	1.98	0.294	
6	35	4.68	0.695	1.85	0.275	
7	35	4.51	0.670	2.32	0.345	
8	35	4.82	0.716	1.88	0.279	
9	35	4.60	0.684	2.19	0.325	
10	35	4.89	0.727	2.38	0.354	
Average (Mean)		4.71	0.700	2.08	0.310	0.443
Standard Deviation		0.121	0.018	0.182	0.027	



**Table III. Horizontal Pull Test Data
Plastic Plate (Cast Acrylic) - Wt. 3.760 lbs**

Trial Number	Arm Orientation α (degrees)	Frictional Force (lb) P_r Fixed Arms	Average Friction Coefficient $\bar{\mu} = P_r / W$	Frictional Force (lb) P_h Hinged Arms	Average Friction Coefficient $\mu_{eff} = P_h / W$	$\mu_{eff} / \bar{\mu}$
1	15	3.09	0.822	0.51	0.136	
2	15	2.93	0.779	0.51	0.136	
3	15	2.89	0.769	0.55	0.146	
4	15	3.26	0.867	0.53	0.141	
5	15	2.55	0.678	0.62	0.165	
6	15	3.52	0.936	0.69	0.184	
7	15	2.89	0.769	0.45	0.120	
8	15	2.92	0.777	0.61	0.162	
9	15	2.89	0.769	0.49	0.130	
10	15	2.32	0.617	0.71	0.189	
Average (Mean)		2.93	0.778	0.57	0.151	0.194
Standard Deviation		0.334	0.089	0.087	0.023	
1	20	2.92	0.777	0.50	0.133	
2	20	2.71	0.721	0.65	0.173	
3	20	3.01	0.801	0.61	0.162	
4	20	3.27	0.870	0.58	0.154	
5	20	2.94	0.782	0.61	0.162	
6	20	3.19	0.848	0.62	0.165	
7	20	3.21	0.854	0.67	0.178	
8	20	3.32	0.883	0.65	0.173	
9	20	3.31	0.880	0.71	0.189	
10	20	3.15	0.838	0.59	0.157	
Average (Mean)		3.10	0.825	0.62	0.165	0.200
Standard Deviation		0.201	0.053	0.057	0.015	
1	25	3.41	0.907	0.98	0.261	
2	25	2.81	0.747	0.98	0.261	
3	25	3.00	0.798	0.82	0.218	
4	25	3.21	0.854	0.83	0.221	
5	25	3.08	0.819	1.00	0.266	
6	25	3.41	0.907	0.88	0.234	
7	25	3.09	0.822	0.96	0.255	
8	25	3.19	0.848	1.06	0.282	
9	25	3.11	0.827	1.00	0.266	
10	25	3.31	0.880	0.91	0.242	
Average (Mean)		3.16	0.841	0.94	0.251	0.299
Standard Deviation		0.186	0.050	0.079	0.021	
1	30	2.99	0.795	1.05	0.279	
2	30	2.71	0.721	1.06	0.282	
3	30	2.91	0.774	1.29	0.343	
4	30	2.91	0.774	1.21	0.322	
5	30	3.01	0.801	1.27	0.338	
6	30	2.92	0.777	1.31	0.348	
7	30	2.91	0.774	1.19	0.316	
8	30	3.18	0.846	1.12	0.298	
9	30	3.19	0.848	1.14	0.303	
10	30	2.98	0.793	1.09	0.290	
Average (Mean)		2.97	0.790	1.17	0.312	0.395
Standard Deviation		0.140	0.037	0.096	0.025	
1	35	2.69	0.715	1.49	0.396	
2	35	2.92	0.777	1.42	0.378	
3	35	3.51	0.934	1.36	0.362	
4	35	3.05	0.811	1.29	0.343	
5	35	3.01	0.801	1.42	0.378	
6	35	3.41	0.907	1.39	0.370	
7	35	3.21	0.854	1.32	0.351	
8	35	3.31	0.880	1.31	0.348	
9	35	2.88	0.766	1.65	0.439	
10	35	3.24	0.862	1.22	0.324	
Average (Mean)		3.12	0.831	1.39	0.369	0.444
Standard Deviation		0.257	0.068	0.120	0.032	

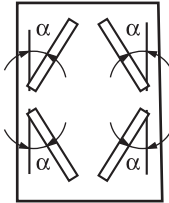
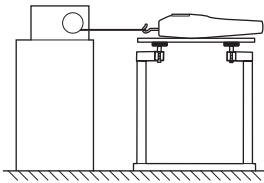
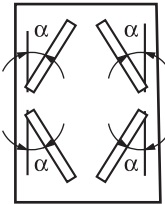
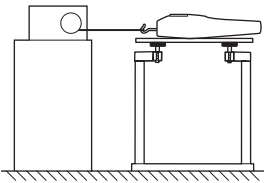


Table IV. Horizontal Pull Test Data
Lubricated Steel Plate/Exxon Superflo 10W-30 - Wt 6.729 lbs

Trial Number	Arm Orientation α (degrees)	Frictional Force (lb) P_r Fixed Arms	Average Friction Coefficient $\bar{\mu} = P_r / W$	Frictional Force (lb) P_h Hinged Arms	Average Friction Coefficient $\mu_{eff} = P_h / W$	$\mu_{eff} / \bar{\mu}$
1	15	1.62	0.241	0.31	0.046	
2	15	1.69	0.251	0.33	0.049	
3	15	1.65	0.245	0.38	0.056	
4	15	1.60	0.238	0.32	0.048	
5	15	1.63	0.242	0.31	0.046	
6	15	1.59	0.236	0.34	0.051	
7	15	1.61	0.239	0.32	0.048	
8	15	1.66	0.247	0.31	0.046	
9	15	1.61	0.239	0.32	0.048	
10	15	1.64	0.244	0.30	0.045	
Average (Mean)		1.63	0.242	0.32	0.048	0.198
Standard Deviation		0.031	0.005	0.023	0.003	
1	20	1.75	0.260	0.42	0.062	
2	20	1.60	0.238	0.40	0.059	
3	20	1.75	0.260	0.43	0.064	
4	20	1.69	0.251	0.49	0.073	
5	20	1.67	0.248	0.45	0.067	
6	20	1.65	0.245	0.42	0.062	
7	20	1.55	0.230	0.46	0.068	
8	20	1.62	0.241	0.43	0.064	
9	20	1.75	0.260	0.45	0.067	
10	20	1.78	0.265	0.40	0.059	
Average (Mean)		1.68	0.250	0.44	0.065	0.260
Standard Deviation		0.077	0.011	0.028	0.004	
1	25	1.60	0.238	0.52	0.077	
2	25	1.75	0.260	0.50	0.074	
3	25	1.53	0.227	0.48	0.071	
4	25	1.59	0.236	0.48	0.071	
5	25	1.72	0.256	0.49	0.073	
6	25	1.67	0.248	0.48	0.071	
7	25	1.62	0.241	0.52	0.077	
8	25	1.53	0.227	0.51	0.076	
9	25	1.68	0.250	0.48	0.071	
10	25	1.62	0.241	0.49	0.073	
Average (Mean)		1.63	0.242	0.50	0.074	0.306
Standard Deviation		0.074	0.011	0.016	0.003	
1	30	1.60	0.238	0.61	0.091	
2	30	1.64	0.244	0.62	0.092	
3	30	1.62	0.241	0.57	0.085	
4	30	1.63	0.242	0.56	0.083	
5	30	1.62	0.241	0.52	0.077	
6	30	1.65	0.245	0.67	0.100	
7	30	1.61	0.239	0.68	0.101	
8	30	1.66	0.247	0.69	0.103	
9	30	1.60	0.238	0.63	0.094	
10	30	1.52	0.226	0.61	0.091	
Average (Mean)		1.62	0.240	0.62	0.092	0.383
Standard Deviation		0.039	0.006	0.055	0.008	



**Table V. Tilt Test Data
Steel Plate - Wt 5.320 lbs**

Trial Number	Arm Orientation α (degrees)	Tilt Angle θ (degrees)	Average Friction Coefficient $\bar{\mu} = \tan(\theta)$	Tilt Angle θ (degrees)	Effective Friction Coefficient $\mu_{eff} = \tan(\theta)$	$\mu_{eff}/\bar{\mu}$
1	15	33	0.649	7	0.123	
2	15	33	0.649	8	0.141	
3	15	33	0.649	8	0.141	
4	15	33	0.649	8	0.141	
5	15	34	0.675	6	0.105	
6	15	33	0.649	9	0.158	
7	15	33	0.649	9	0.158	
8	15	33	0.649	8	0.141	
9	15	33	0.649	8	0.141	
10	15	33	0.649	8	0.141	
Average (Mean)		33.1	0.652	7.9	0.139	0.213
Standard Deviation		0.316	0.008	0.876	0.016	
1	20	37	0.754	14	0.249	
2	20	37	0.754	11	0.194	
3	20	37	0.754	11	0.194	
4	20	38	0.781	6	0.105	
5	20	38	0.781	10	0.176	
6	20	36	0.727	8	0.141	
7	20	36	0.727	8	0.141	
8	20	38	0.781	11	0.194	
9	20	36	0.727	10	0.176	
10	20	37	0.754	11	0.194	
Average (Mean)		37.0	0.754	10.0	0.177	0.235
Standard Deviation		0.816	0.022	2.211	0.040	
1	25	35	0.700	13	0.231	
2	25	36	0.727	15	0.268	
3	25	35	0.700	12	0.213	
4	25	35	0.700	12	0.213	
5	25	35	0.700	13	0.231	
6	25	35	0.700	15	0.268	
7	25	33	0.649	13	0.231	
8	25	35	0.700	10	0.176	
9	25	33	0.649	11	0.194	
10	25	34	0.675	13	0.231	
Average (Mean)		34.6	0.690	12.7	0.226	0.328
Standard Deviation		0.966	0.025	1.567	0.029	
1	30	35	0.700	16	0.287	
2	30	34	0.675	16	0.287	
3	30	31	0.601	17	0.306	
4	30	34	0.675	15	0.268	
5	30	35	0.700	16	0.287	
6	30	35	0.700	15	0.268	
7	30	33	0.649	14	0.249	
8	30	32	0.625	16	0.287	
9	30	34	0.675	16	0.287	
10	30	34	0.675	15	0.268	
Average (Mean)		33.7	0.667	15.6	0.279	0.418
Standard Deviation		1.337	0.033	0.843	0.016	
1	35	34	0.675	21	0.384	
2	35	32	0.625	17	0.306	
3	35	33	0.649	16	0.287	
4	35	32	0.625	19	0.344	
5	35	33	0.649	17	0.306	
6	35	33	0.649	17	0.306	
7	35	34	0.675	16	0.287	
8	35	34	0.675	17	0.306	
9	35	34	0.675	19	0.344	
10	35	33	0.649	16	0.287	
Average (Mean)		33.2	0.655	17.5	0.316	0.482
Standard Deviation		0.789	0.020	1.650	0.032	

